Journal of Low Temperature Physics, Vol. 142, Nos. 3/4, February 2006 (© 2006)
DOI: 10.1007/s10909-006-9114-y

Neutron-Scattering Evidence for a Spin-Peierls Ground State in $(TMTTF)_2PF_6$

J.-P. Pouget[a], P. Foury-Leylekian[a], D. Le Bolloc'h[a], B. Hennion[b], S. Ravy[c], C. Coulon[d], V. Cardoso[a], and A. Moradpour[a]

[a]Laboratoire de Physique des Solides, CNRS UMR 8502, Université Paris Sud, 91405 Orsay, France
[b]Laboratoire Léon Brillouin,CNRS UMR 12, CEA Saclay, 91191 Gif-sur Yvette, France
[c]Synchrotron SOLEIL, L'Orme des Merisiers, Saint Aubin BP48, 91192 Gif-sur Yvette, France
[d]CRPP, CNRS UPR 8641, Université Bordeaux I, 33600 Pessac, France.

$(TMTTF)_2X$, with $X=PF_6$, exhibits, at T_{SP}, a spin-Peierls transition. Below T_{SP} elastic neutron scattering measurements performed on large protonated and deuterated samples reveal the formation of very weak superstructure reflections at the (1/2,1/2,1/2) reduced wave vector. Upon deuteration T_{SP} decreases by 30% while the charge ordering (CO) transition increases by 25%. In this framework we stress the importance of the anions, X, and of their organic cavities to stabilize the CO transition of the $(TMTTF)_2X$ salts.
PACS numbers: 71.27+a, 71.45 Lr, 77.80 Bh.

1. INTRODUCTION

The quasi-1D conductors $(TMTTF)_2X$ and $(TMTSF)_2X$, made of slightly dimerized zig-zag stacks of TMTTF and TMTSF whose methyl groups delimit cavities in which monovalent X anions are located, present a remarkable sequence of competing ground states ranging from spin-Peierls (SP) pairing, antiferromagnetism (AF) / spin density wave, and then superconductivity. Recently, the discovery[1,2] in the $(TMTTF)_2X$'s of a $4k_F$ charge ordered (CO) state at the critical wave vector $\mathbf{q}^F_{CO}=(0,0,0)$, while allowing one to understand older results[3], sheds a new light on the phase diagram of this series. This finding calls for a better knowledge of the low temperature structures of the TMTTF salts, especially the SP ones.

Since its first report 25 years ago[4] very little is known on the SP lattice distortion of $(TMTTF)_2PF_6$ because of the extreme sensitivity of TMTTF to X-ray irradiation damages. With the successful growth of large ($\sim 20mm^3$) single crystals we were able to perform for the first time elastic neutron

scattering investigations of the SP superstructure both in protonated and 98% deuterated $(TMTTF)_2PF_6$: $PF_6(H_{12})$ and $PF_6(D_{12})$ respectively.

2. THE SPIN-PEIERLS TRANSITION OF $(TMTTF)_2PF_6$

The magnetism of $(TMTTF)_2X$ has been characterized by SQUID and EPR measurements performed on samples taken from the same batches as those used for the neutron scattering investigation. Figure 1 shows the thermal dependence of the spin susceptibility, χ_s, of the $PF_6(H_{12})$, $PF_6(D_{12})$ and $AsF_6(H_{12})$ salts. The SP transition of $PF_6(H_{12})$, $PF_6(D_{12})$ and $AsF_6(H_{12})$ determined from the maximum of slope $d\chi_s/dT$ in the drop of χ_s, occurs respectively at T_{SP} = 16.4K, 12.9K and 11.1K and opens below T_{SP} a singlet-triplet gap (defined by $\chi_s \sim T^{-1}\exp(-\Delta/T)$ of Δ = 79K, 75K and 70K. Interestingly, figure 1 shows that T_{SP} and Δ of $PF_6(D_{12})$ are intermediate between those of $PF_6(H_{12})$ and $AsF_6(H_{12})$.

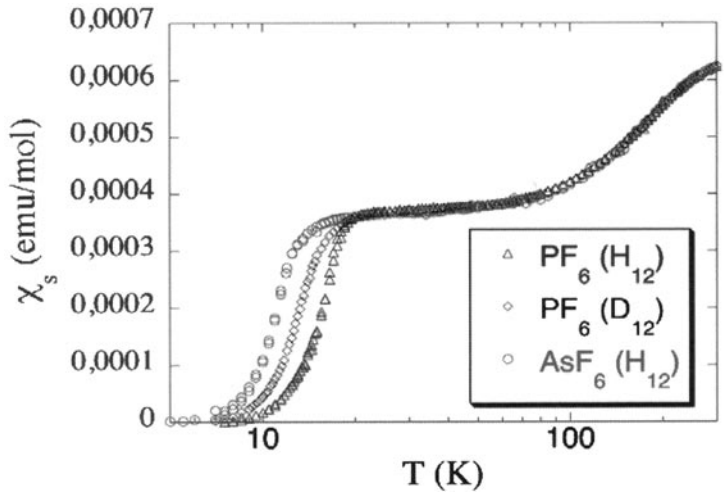

Fig. 1. SQUID measurement of the spin susceptibility of $(TMTTF)_2PF_6$ (H_{12})-triangle, $PF_6(D_{12})$-lozenge and $AsF_6(H_{12})$-circle as a function of logT.

Elastic neutron scattering measurements, performed in the conditions described in ref.5, provide a clear identification of a superstructure formation through the detection of several very weak satellite reflections at the $\mathbf{q_{SP}}$ = (1/2,1/2,1/2) reduced wave vector. Figure 2 shows typical scans through the (2.5,0.5,-0.5) reflection of $(TMTTF)_2PF_6(D_{12})$. In particular, the longitudinal scan shows the doubling of chain periodicity expected from the SP pairing of localized spins ½ (one per TMTTF dimer) into non magnetic singlets. The

intensity of the SP reflections, ~0.23c/s, is about $3x10^{-4}$ smaller than that of the main Bragg reflections. Figure 3 shows that the SP reflection of the PF_6 (D_{12}) vanishes at 13K, which nicely corresponds to T_{SP} deduced from

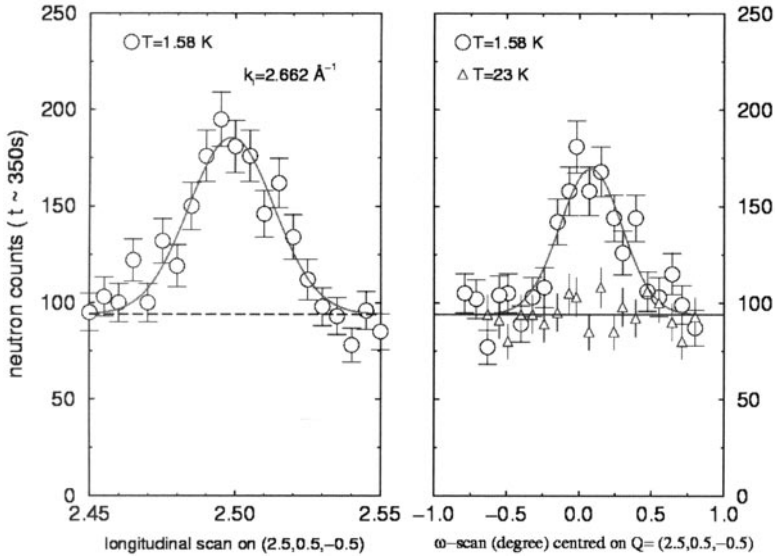

Fig.2. Longitudinal a* scan (left) and transverse ω scan (right) at 1.58K (circle) through the (2.5,0.5,-0.5) superstructure reflection of the main twin (75% of the volume) of a $(TMTTF)_2PF_6$ (D_{12}) crystal of $22mm^3$. The ω scan shows the vanishing of the SP reflection above T_{SP} at 23K (triangle).

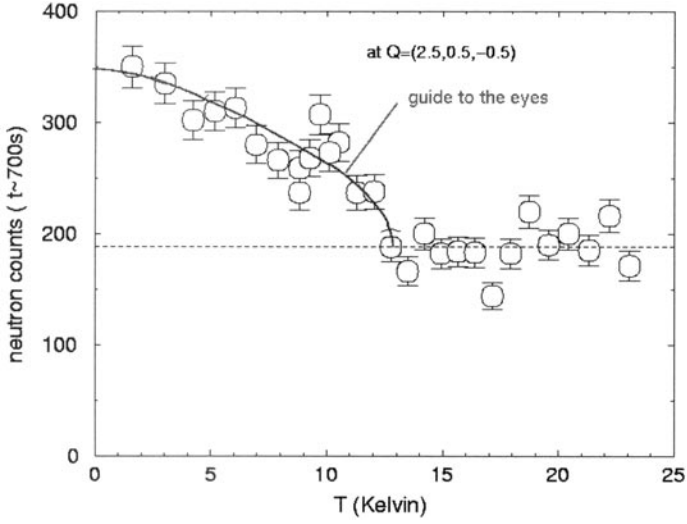

Fig.3. Thermal dependence of the peak intensity of the (2.5,0.5,-0.5) superstructure reflection in $(TMTTF)_2PF_6$ (D_{12}).
magnetic measurements. Similar results were obtained from $(TMTTF)_2PF_6$ (H_{12})[5], but because of the presence of a high background due to the incoherent scattering from the H, the SP reflections are not so easily detected. However their intensity vanishes at T_{SP}=18±1K, which is higher than T_{SP} of PF_6 (D_{12}).

3. THE CHARGE ORDERING TRANSITION

As already pointed out in ref. 6,7, the decrease of T_{SP} must be related with the increase of T_{CO} because the stabilization of a $4k_F$ on-site charge modulation weakens the $2k_F$ bond response driving the SP instability. In order to determine the CO transition of our samples we have deduced, using the calculation of ref. 8, the effective conductivity σ_n from the observed EPR line asymmetry. Log σ_n when plotted as a function of 1/T (figure 4), shows that the gap of charge significantly increases below 69K, 90K and 100K in PF_6 (H_{12}), PF_6 (D_{12}) and AsF_6 (H_{12}) respectively. In the H_{12} compounds, the change of slope of log σ_n occurs at T_{CO} of the CO[1]-ferroelectric[2] transition.

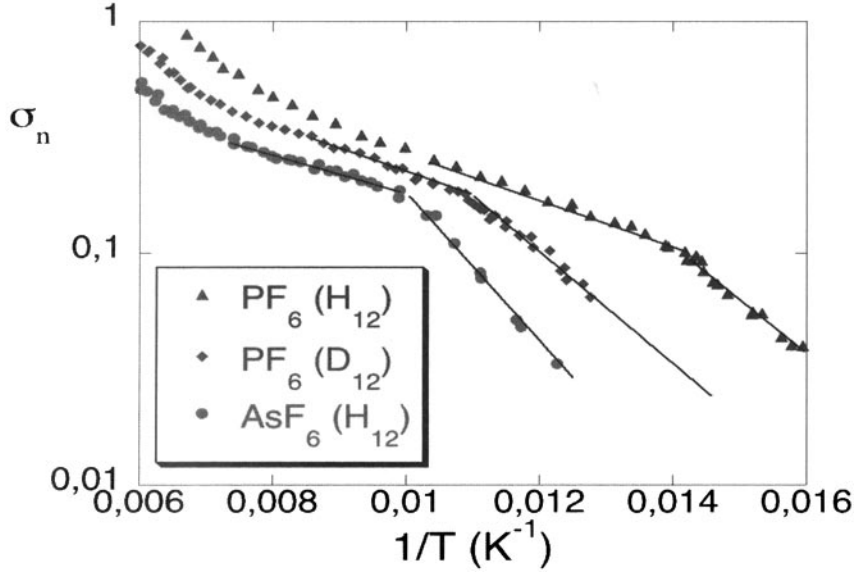

Fig. 4. Log σ_n as a function of T^{-1} in $(TMTTF)_2PF_6$ (H_{12})-triangle, PF_6 (D_{12})-lozenge and AsF_6 (H_{12})-circle. The conductivity scale is arbitrary.

4. DISCUSSION

From our data one deduces the approximate linear relationship:

$$T_{sp} \approx 30K - 0.19\ T_{CO}. \quad (1)$$

The rate of variation dT_{SP} / dT_{CO} given by (1) is somewhat comparable to the one found in pressurized $(TMTTF)_2AsF_6$[9]. Expression (1) shows that in the absence of CO, T_{sp} could be higher than 30K. Such T_{sp} are reached in $(BCPTTF)_2PF_6$ and AsF_6 stabilizing the same q_{SP}[10]. Expression (1) leads also to a vanishing of T_{sp} for $T_{CO} \approx 160K$. In $(TMTTF)_2SbF_6$ and SCN[3], presenting a CO transition at about this T_{CO}, the ground state has shifted from SP to AF.

With respect to PF_6 (H_{12}) deuteration depresses T_{SP} by 30% through an enhancement of T_{CO} by 25%. Deuteration acts on T_{CO} like a negative pressure probably via the increase of the volume of the anion cavity delimited by the methyl groups, since the C-D bond length is smaller than the C-H one by ~0.01Å. A similar isotopic effect has been reported in the AsF_6 and SbF_6 salts[11]. T_{CO} depends upon the nature of the anion as well as upon its free volume in the organic cavities, as illustrated by Figure 5 which plots T_{CO} as a function of the anion X quantified by its mass M_X. For anions of same symmetry, T_{CO} increases with M_X, as well as with the anion size which controls the electron-anion coupling α. T_{CO} increases also with the misfit between the anion shape and the inner shape of the organic cavity; for example along the sequence of successively less symmetric anions: Br, BF_4,

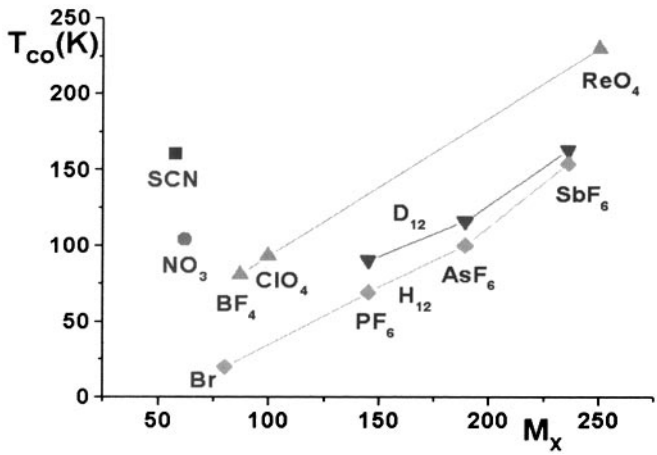

Fig. 5. CO transition temperature T_{CO} at ambient pressure (taken from ref. 1,2,3,6,11 and this work) as a function of the anion mass M_X. For X = NO_3, BF_4 and ClO_4, T_{CO} is identified at the temperature at which there is, from the T^{-1} dependence of the thermopower[12], a large increase of the gap of charge. For X = Br, T_{CO} is taken in the 18-25K temperature range where the activation energy of the conductivity and of the thermopower increases.

NO_3, SCN having about the same M_X. In other words T_{CO} appears to increase when the potential experienced by the anion in its organic cavity is flatter (i.e. when its second derivative V'' is smaller). Deuteration (pressure) decreases (increases) V''. These features mean that the anions control the CO process probably because their shift from the inversion center of the organic cavities stabilizes the charge disproportion on their two first neighboring TMTTF molecules (for a microscopic calculation see ref. 7).

In this framework, the CO transition can be described as a $4k_F$-Peierls transition in which structural degrees of freedom (which remain to be determined for $\mathbf{q}^{\mathbf{F}}_{CO}$[6,13], but which are identified for the $\mathbf{q}^{\mathbf{AF}}_{CO}$=(0,1/2,1/2) order of X=SCN[13]) are coupled (via the electron-phonon/anion coupling α) to the $4k_F$ electron-hole response of the stack. If one assumes for simplicity that this response diverges, as for a spinless fermion gas, like:

$$\chi(4k_F,T) \sim N(E_F^*) \ln(E_C^*/k_BT), \quad (2)$$

one obtains, in the mean field approximation and for a commensurability 2, a $4k_F$-Peierls transition at:

$$k_BT_{CO} \approx E_C^* \exp\text{-}(2\lambda)^{-1}, \quad (3)$$

where $N(E_F^*)$ is the density of state of the spinless fermions and $\lambda = N(E_F^*)\alpha^2/\hbar\Omega$ is the reduced electron-phonon/anion coupling constant. Here, Ω is the frequency of the bare phonon mode coupled to the TMTTF's charge. If the CO transition is controlled by a local displacement of the anions in their cavity, one simply has $\Omega^2 = V''/M_X$. In this crude model T_{CO}, depends upon the nature of the anion and of its cavity through the quantities α, V'' and M_X entering in the dimensionless constant λ.

REFERENCES

1. D.S. Chow et al, *Phys. Rev. Lett.* **85**, 1698 (2000).
2. P. Monceau et al, *Phys. Rev. Lett.* **86**, 4080 (2001).
3. C. Coulon, *J. Phys. IV France* **114**, 15 (2004) and references there in.
4. J.-P. Pouget et al, *Mol .Cryst. Liq. Cryst.* **79**, 129 (1982).
5. P. Foury-Leylekian et al, *Phys. Rev. B* **70**, 180405(R) (2004).
6. P. Foury-Leylekian et al, *Physica B* **312**, 574 (2002).
7. J. Riera and D. Poilblanc, *Phys. Rev. B* **63**, 241102(R) (2001).
8. J.H. Pifer and R. Magno, *Phys. Rev. B* **3**, 663 (1971). This theory linking the EPR lineshape to the skin depth $\sim\sigma^{-1/2}$ has been adapted to the case of anisotropic conductors to account for the measurements in the TMTTF's.
9. F. Zamborsky et al, *Phys. Rev. B* **66**, 081103(R) (2002).
10. Q. Liu et al, *Synth. Met.* **56**,1840 (1993).
11. T. Nakamura et al, *Synth. Met.* (in press).
12. K. Mortensen et al, *Phys. Rev. B* **28**, 5856 (1983).
13. Y. Nogami and T. Nakamura, *J. Phys. IV France* **12**, Pr9-145 (2002).